Vibrational Coupling of Nearly Degenerate Electronic States

WALTER E. BRON AND MAX WAGNER*
IBM Watson Research Center, Yorktown Heights, New York

(Received 28 December 1965)

An anomalously large interval between lines of a vibrational series has been observed in the vibronic part of the absorption spectra of NaCl, KCl, and RbCl containing Eu^{2+} ions. Many details of these anomalous spectra can be accounted for through a vibrational coupling of two nearly degenerate excited electronic states, each belonging to a different electronic configuration. The analysis of the vibrational coupling is simplified by the fact that the point symmetry of the rare-earth defect admits only nondegenerate states. Consequently, a theorem by Neumann and Wigner requires that any two electronic states may not cross each other under variations of one vibrational coordinate, although they may approach each other. Furthermore, the Born-Oppenheimer approximation applies, if it is assumed that the states do not approach each other by less than a typical vibrational quantum. Under these circumstances, the vibrational potential can be defined for each of the pertinent electronic states, and the corresponding vibronic spectra determined in detail. It is shown that one of the coupled states has associated with it a strongly increased vibrational frequency. In addition, the selection rule $\Delta m=0, \pm 2\cdots$ applies for absorptive transitions to the vibrational components of this state. Together these facts account for the observed anomalous line interval. The other coupled state has associated with it a decreased vibrational frequency. However, the transition probability to this state is shown to be very small, in agreement with the fact that the corresponding transitions are not observed experimentally. The observed emission spectrum is also accounted for in the analysis.

INTRODUCTION

VIBRONIC spectra have recently been observed in alkali-halide crystals containing rare-earth impurities (Eu^{2+}, Sm^{2+}, or Yb^{2+}). A number of papers by the authors[1-3] treat in detail the theory of these spectra and an analysis of the experimental results. Vibronic spectra accompanying electronic transitions of the type $4f^n \rightleftarrows 4f^{n-1}5d$ are shown to predominantly reflect the existence of pseudolocalized vibrations, which arise because of the presence of the defect.[1,2] Table I briefly summarizes all the observed vibrational frequencies of the pseudolocalized type. In contrast, vibronic spectra accompanying electronic transitions of the type $4f^n \rightleftarrows 4f^n$ may reflect predominantly nonlocalized vibrations.[3] In this paper we are concerned with an experimentally observed vibrational frequency, of the pseudolocalized type, which is anomalously high.

It has been shown that the point symmetry of the rare-earth defect is C_{2v}.[4] This point group has only one-dimensional representations. It should be realized that, as a consequence, only nondegenerate electronic or vibrational states may be associated with this defect. Two major pseudolocalized frequencies are present, one corresponding to a vibrational mode of A_1 symmetry, the other to a mode of B_1 symmetry.[1] (Two minor pseudolocalized modes of the same symmetry also occur, but prove to be of lesser importance here.)

Nondegenerate electronic states can only couple to A_1 modes.[2] (The two observed frequencies tabulated in Table I, correspond to the major and minor A_1 vibrational modes noted above.) It is for this reason that, in general, the vibrational frequencies associated with absorptive and emissive transitions within one host lattice are essentially the same. However, a striking exception to this rule is observed in the spectra of Eu^{2+} in the alkali chlorides (NaCl, KCl, RbCl), where the vibrational line interval observed on the low-energy tail of the first broad absorption band is strongly increased over that on the corresponding emission band (see Table I).

We are led to ascribe this behavior to the dynamics of nearly degenerate electronic states which are coupled and mixed by the vibrations. Nearly degenerate electronic states may not only couple to the A_1 mode, but also to the B_1 mode. But exact degeneracy being forbidden by symmetry, the electronic levels cannot cross each other by a theorem due to Neumann and Wigner.[5]

It is this theorem which provides a useful basis for our investigation. In contrast to the pure Jahn-Teller case, where symmetry allows full degeneracy of the

TABLE I. Vibronic frequencies in rare-earth-doped alkali halides.[a]

	NaCl		KCl		RbCl		KBr		KI	
	ω_1	ω_2	ω_1	ω_2	ω_1	ω_2	ω_1	ω_2	ω_1	ω_2
	Absorption (First excited state)									
Sm^{2+}	215	52	208	23	193	27	115	39	85	56[b]
Eu^{2+}	216	54	206		191	36	116	37	86	24
	(793)[c]		(822)[c]		(831)[c]					
Yb^{2+}	218		208	43	185		114		84	
	Emission (ground state)									
Eu^{2+}	210	48	196	45	183	36	110	37	79	19
Yb^{2+}	208	45	203	44	183	42	108	37	79	19

[a] Frequencies given in cm^{-1}.
[b] Probably $2\omega_2$.
[c] These are apparent frequencies, i.e., those obtained from the observed large line interval in the vibronic spectra. The actual frequency is, as shown in the text, equal to half this value.

* Present address: Institut für Theoretiche und Angewandte, Physik der Technischen Hoschschule, Stuttgart, Germany.

[1] M. Wagner and W. E. Bron, Phys. Rev. **139**, A223 (1965).
[2] W. E. Bron and M. Wagner, Phys. Rev. **139**, A233 (1965).
[3] W. E. Bron, Phys. Rev. **140**, A2005 (1965).
[4] W. E. Bron and W. R. Heller, Phys. Rev. **136**, A1433 (1964).
[5] J. von Neumann and E. Wigner, Physik Z. **15**, 467 (1929).

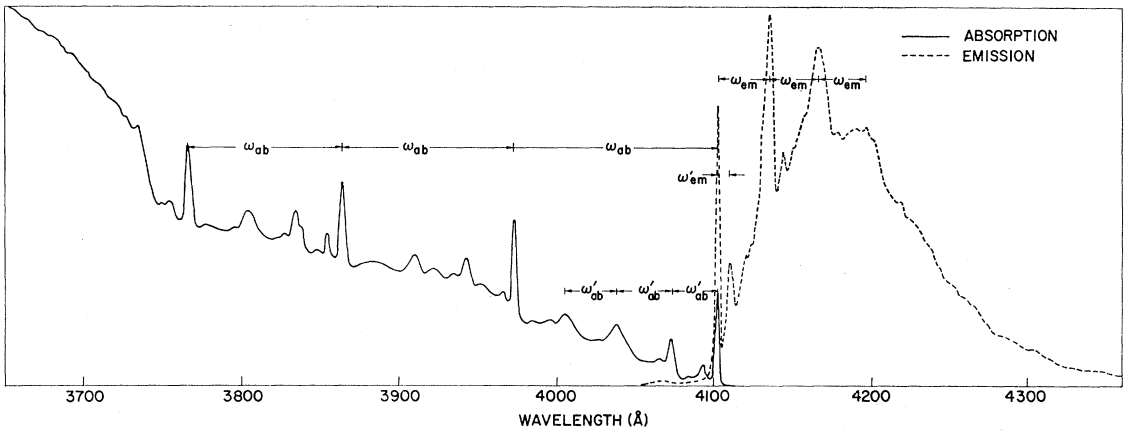

FIG. 1. Vibronic structure on the tail of the lowest energy absorption band and the emission band of the system KCl:Eu^{2+} at 10°K.

electronic states, in our case we may assume that the states remain sufficiently separated to suppress a "Born-Oppenheimer violation." Thus, as will be seen, the potential curves of (say) the B_1 mode separate into one of high effective frequency and one of a lower frequency, which latter proves to be less significant. A further increase of the apparent vibronic frequency follows from the approximate selection rule $\Delta m = 0, \pm 2$, which is a consequence of the special type of coupling to the B_1 mode.

We shall refer to the present case as a dynamical "pseudo-Jahn-Teller-effect," because it is a consequence of the dynamical coupling of nearly degenerate electronic states. It should be emphasized that there exists particularly suitable circumstances in the present case, which make the effect much stronger than in most cases of the pure Jahn-Teller effect, where the vibrational frequency in absorption spectra is essentially the same as in emission spectra.[6]

TABLE II. Vibronic lines on the lowest energy absorption and on the emission bands of Eu^{2+}:KCl.

	Absorption		
λ (Å)	ν (cm^{-1})	ω_{ab} (cm^{-1})	ω_{ab}' (cm^{-1})
4108.2	24 341.6		
4073.7	24 547.7		206.1
4039.6	24 754.9		207.1
4007.7	24 952.0		197.1
3974.0	25 163.6	822.0	
3942.0	25 367.8		204.2
3910.0	25 575.4		208.6
3884.7	25 742.0		166.6
3864.5	25 876.6	713.0	
3834.5	26 079.0		203.4
3804.5	26 284.7		205.7
3767.8	26 540.7	664.1	

	Emission	
λ (Å)	ν (cm^{-1})	ω_{em} (cm^{-1})
4108.2	24 341.6	
4141.4	24 146.4	195.2
4173.0	23 963.6	184.8
4203.8	23 788.0	175.6

EXPERIMENTAL RESULTS

Experimental methods have been described in Ref. 4. Figure 1 shows the vibronic structure in the lowest energy absorption and emission bands of Eu^{2+}:KCl at 10°K and indicates the major line interval in absorption (ω_{ab}) and emission (ω_{em}). A minor line interval (ω_{ab}', ω_{em}') is also discernible in the spectra.

Table II lists the corresponding vibrational frequencies ω_{ab}, ω_{ab}' and ω_{em}. Comparison of Fig. 1 and Table II with Table I shows that ω_{em} corresponds to ω_1, ω_{em}' with ω_2 in the emission data for KCl, and ω_{ab}' with the normal frequency ω_1 observed in the absorption spectra of Sm^{2+} and Yb^{2+} in KCl. In comparison with ω_1 for Sm^{2+} and Yb^{2+} in the alkali chlorides, ω_{ab} is anomalously large, it being approximately four times ω_1. Also the interval ω_{ab} decreases monotonically at a faster rate than does ω_{ab}'. Nearly identical results are obtained in Eu^{2+}:NaCl and Eu^{2+}:RbCl. For simplicity, in the following discussion, we restrict ourselves to the case of Eu^{2+}:KCl.

The four sharp, intense lines in the absorption spectra of Eu^{2+}:KCl are indicated in Fig. 2 as the four sharp levels in the middle energy diagram. The shaded areas in this figure indicate the location of the broad bands observed in the absorption spectrum of this material. For comparison, a similar energy diagram is given for Eu^{2+}:CaF_2 and Eu^{2+}:KBr. In the latter spectrum, shown in detail in Fig. 3, a number of sharp lines also appear below the lowest energy broad absorption band. Each sharp line is followed by a series of vibronic lines spaced at the normal interval indicated in Table I. Unlike the case of Eu^{2+}:KCl, where the vibronic series with interval ω_{ab} are separated, in Eu^{2+}:KBr these series interweave, i.e., the first line of one starts before

[6] H. C. Longuet-Higgins, U. Öpik, M. H. L. Pryce, and R. A. Sack, Proc. Roy. Soc. (London) A244, 1 (1958).

the last line of the preceding series (as indicated by the horizontal cords in Fig. 3). The separation between the first lines of each series is of the order of 350 cm^{-1}, i.e., less than one-half that between the intense sharp lines in Eu^{2+}:KCl.

DISCUSSION

We consider first the possibility that the four sharp, intense lines observed in the absorption spectra of Eu^{2+}:KCl at 24 341.6, 25 163.6, 25 876.6, and 26 540.7 cm^{-1} represent simply transitions to four different pure electronic states ("zero-phonon states") of the excited $4f^7$ configuration or the excited $4f^6 5d$ configuration of the Eu^{2+} ion. We show that this is unlikely for Eu^{2+} in the alkali chlorides.

The remainder of the discussion is concerned with an analysis of the vibrational coupling of two nearly degenerate electronic states of opposite parity, and we show that many features of the observed spectra of Eu^{2+}:KCl can be interpreted in terms of this vibrational interaction.

I. Electronic States

It is possible to make reasonable guesses about the character of the electronic states taking part in the transitions, through a comparison of the spectra of Eu^{2+} in KCl, KBr, and CaF_2. We first realize that the sharp lines of the Eu^{2+} spectra in the 25 000 cm^{-1} region of Fig. 2 cannot belong to pure $4f \rightarrow 4f$ transitions, because the strengths of such transitions would be approximately 10^3 times smaller[7] than those observed. It is equally unlikely, that the observed intense lines arise from an admixture of $4f^{n-1}5d$ states to $4f^n$ states. Such admixture is limited by the ratio of the appropriate crystal-field matrix elements, typically of the order of 10^2 cm^{-1},[4] and the energy difference between the states, which according to Fig. 2 is at least of the order of 10^3 cm^{-1}. Hence, we may conclude that the observable transitions are to excited states which are not primarily of the $4f^7$ configurations, but of the $4f^6 5d$, $4f^6 6s$, etc., configurations. By an analysis due to Dieke *et al.*[8] the lowest energies belong to the $4f^6 5d$ configuration whereas, as noted earlier, the ground states are of the $4f^7$ configuration.

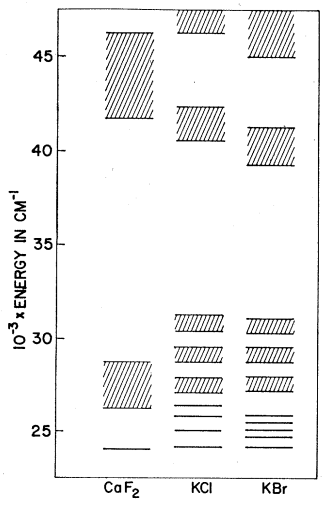

FIG. 2. The major absorption lines and bands for the systems KCl:Eu^{2+}, CaF_2:Eu^{2+}, and KBr:Eu^{2+}.

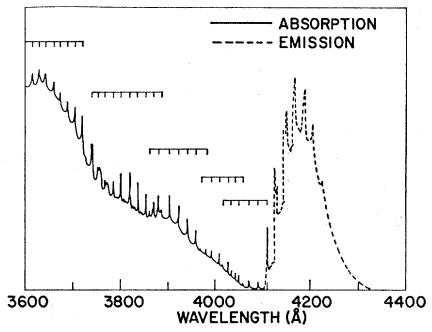

FIG. 3. Vibronic structure on the tail of the lowest energy absorption band and the emission band of the system KBr:Eu^{2+} at 10°K.

Let us consider in more detail the excited state. The $4f^6$ core of this state has a ground multiplet with states[9]

$$^7F_0, ^7F_1, ^7F_2 \cdots . \tag{1}$$

These are descendents from ^7F via spin-orbit splitting, which is typically of the order of 350 cm^{-1}. The crystal-field splitting of the $4f^6$ configuration is of the order of 20 to 50 cm^{-1} (Ref. 4) and may be neglected against the spin-orbit separations. The single $5d$ electron separates from the six $4f$ electrons. In the $5d$ shell, the spin-orbit coupling is smaller than the crystal field splitting, which latter is usually assumed to be of the order of 10^4 cm^{-1} [10] in ionic crystals. Therefore, the spin-orbit coupling is too weak to mix different crystal field states determined by the orbital angular momentum of the $5d$ electron. Accordingly, the "block" representation for this electron is

$$D^{(2)} D_{1/2}, \tag{2}$$

where $D^{(2)}$ refers to the reducible representation of the parent state with orbital angular momentum of two, and $D_{1/2}$ to the spin representation.

The wave function for the single $5d$ electron is a product of a spin function, $\sigma_{s,m_s}(\zeta)$, defined in spin space $\zeta_1 \cdots \zeta_7$, and a function ψ which depends only on

[7] See, for example, the observed intensities for such transitions as determined for the isoelectronic Gd^{3+} ion by G. Freed and S. Katcoff, Physica **14**, 17 (1948).

[8] G. H. Dieke, H. M. Crosswhite, and B. Dunn, J. Opt. Soc. Am. **51**, 820 (1961).

[9] D. S. McClure, *Solid State Physics*, edited by F. Seitz and D. Turnbull (Academic Press Inc., New York, 1959), Vol. 9, p. 399 ff.

[10] See, for example, D. L. Wood and W. Kaiser, Phys. Rev. **126**, 2079 (1962); E. Patscheke, dissertation, 1964, Tech. Hochschule Stuttgart (unpublished); W. Moffit, G. L. Goodman, M. Fred, and B. Weinstock, Mol. Phys. **2**, 109 (1959).

the electronic position r_i

$$\psi_{l,m_l}(r_7)\sigma_{s,m_s}(\zeta), \tag{3}$$

where l, m_l, s, and m_s have their usual meaning and l and s have the values 2 and $\frac{1}{2}$, respectively, and the subscript 7 refers to the coordinates of the $5d$ electron.

In C_{2v} symmetry, the orbital part of (3) is decomposed into the representations;

$$D^{(2)}=2A_1+A_2+B_1+B_2 \tag{4}$$

whereas, the spin representation $D_{1/2}$ is not split by the crystal field. Thus, the $5d$ electron has the wave functions

$$\psi_\mu(r_7)\sigma_{1/2,m_s}(\zeta_7), \quad \mu=A_1, A_2, B_1, B_2. \tag{5}$$

The total wave function of the $4f^6 5d$ configuration is, therefore of the form

$$\phi_j(r_1\cdots r_6,\zeta_1\cdots\zeta_6)\psi_\mu(r_7)\sigma_{1/2,m_s}(\zeta_7), \tag{6}$$

where j indicates the series of relatively closely spaced ^7F_J states of the spin-orbit-split core configuration. Since the crystal-field splitting exceeds the splitting of the sharp states of Eu^{2+}:KBr (see Fig. 2), we infer that we are concerned here with only one of the representations μ given by (4). The separation of the first 5 excited states of Eu^{2+} in KBr must therefore be completely due to the spin-orbit splitting of the $4f^6$ configuration. The magnitude of this splitting should not depend strongly on the host crystal. That is, the splitting for Eu^{2+}:KCl should approximate that for Eu^{2+}:KBr. This is evidently not the case (see Fig. 2).

To account for the anomalously large spacing between the sharp lines in the system Eu^{2+}:KCl and also for the monotonic decrease of this spacing (Fig. 1) we propose an explanation based on a strong vibrational coupling of one of the states (6) to another electronic state, which belongs to the $4f^7$ configuration and, therefore, is not normally optically active. Under this interpretation, the four sharp lines of Eu^{2+}:KCl, Eu^{2+}:NaCl, and Eu^{2+}:RbCl are not associated with pure electronic states, but are part of a *vibronic series*. It will be shown that a considerable part of the experimental data can be accounted for in this way. We shall develop this interpretation in more detail in the next section.

Before proceeding we write, in analogy to Eqs. (1)–(6) the corresponding terms for the ground configuration. This configuration consists of a half-filled $4f$ shell. Its parity (in free space) is odd. It has been established by Freed and Katcoff[7] and others[11] that the ground state is a $^8S_{7/2}$ state. Being an S state, its wave function may be written as a product

$$\psi_{L,m_L}(r)\sigma_{S,m_S}(\zeta), \tag{7}$$

where L and S have the values 0 and $\frac{7}{2}$, respectively. In C_{2v} symmetry (7) may be written as

$$\psi_{A_1}(r)\sigma_{7/2,m_s}(\zeta), \tag{8}$$

where A_1 refers to the totally symmetric irreducible representation of the state in real space. The product (8) is an adequate description because the spin-orbit coupling is weak for an $L=0$ state. The crystal field acts only on the spatial coordinates $r_1\cdots r_7$. As a consequence, the spin representation Γ of $\sigma(\zeta)$ remains degenerate. For perturbing fields which act only on the spatial coordinates it is, therefore, not necessary to use the double-valued representations of C_{2v}. Although, of course, the total electronic state belongs to the double-valued representation $D_{1/2}$ of C_{2v} ,which also holds true for the excited state.

II. Electron-Lattice Interaction

(a) *Selection Rules for Nondegenerate States*

The coupling of the ground state (8) to lattice vibrational modes is given by the matrix element[1–3]

$$\int\psi_{A_1}^*(r)V^{(\gamma)}(r)\psi_{A_1}(r)d\tau\int\sigma_{7/2,m_S}(\zeta)\sigma_{7/2,m_S}(\zeta)d\zeta, \tag{9}$$

where $V^{(\gamma)}(r)$ is the coupling function in r space,[12] and γ is a (single-valued) representation of C_{2v}. From (9) it is clear that

$$\gamma=A_1, \tag{10}$$

i.e., the ground state (8) couples only to A_1 modes of the lattice. However, this coupling is very weak, since among other things, the state (8) is shielded by the $5s^25p^6$ electrons and does not interact strongly with lattice vibrations.

In order to determine the coupling of the excited state (6) to the lattice modes, we take account of the fact that the $4f^6$ configuration of the core is also strongly localized at the nucleus of the rare-earth ion and shielded from the crystal potential. Consequently, the vibrational coupling function $V^{(\gamma)}(r_1\cdots r_7)$ does not depend strongly on $r_1\cdots r_6$. We may, accordingly, average over these coordinates, and define an effective coupling function $V^{(\gamma)}(r_7)$ which depends principally on the $5d$ electron. Then the matrix element for the coupling is given by

$$\int\phi_j^*\phi_j dr_1\cdots r_6 d\zeta_1\cdots\zeta_6\int\sigma_{7/2,m_S}^*\sigma_{7/2,m_S}d\zeta_7 \times\int\psi_\mu^*(r_7)V^{(\gamma)}(r_7)\psi_\mu(r_7)dr_7 \tag{11}$$

which differs from zero only if

$$\gamma=A_1 \tag{12}$$

[11] See, for example, W. F. Meggers, Rev. Mod. Phys. **14**, 96 (1942).

[12] $V^{(\gamma)}$ corresponds to U_k in Refs. 2 and 3. A more uniform presentation is obtained here if the $V^{(\gamma)}$ notation is used.

which reflects the general result that nondegenerate electronic states can couple only to A_1 lattice modes.

(b) Vibrational Coupling of Nearly Degenerate States

It may be inferred from the calculations by Judd,[13] and from the spectrum of Gd^{3+},[5] that some excited states of the $4f^7$ configuration (hereafter designated $4f^6 4f^*$) lie in the neighborhood of the lowest states of the $4f^6 5d$ configuration of Eu^{2+}. In order to account for the experimental results, we next investigate the case where two states, one from each configuration, approach each other so closely that a strong vibrational coupling arises. This situation is similar to that of the Jahn-Teller effect,[14] but instead of truly degenerate electronic states, which are nonexistent in C_{2v} symmetry, the states here are almost degenerate. Both configurations, $4f^6 4f^*$ and $4f^6 5d$, are then mixed by the dynamical coupling function $V^{(\gamma)}(r)$ as well as by the static crystal field $V^{(c)}(r)$. This mixing appears in r space and we may assume that it is much stronger than the spin-orbit coupling in each configuration, whence we may neglect the spin-orbit interaction. It is clear that this assumption has to be investigated in more detail for the $4f^6 4f^*$ states, although it has been demonstrated in Sec. I for the ground state and for the states of the $4f^6 5d$ configuration. We defer a study of this point for future work, as it would blur the clear features of the following calculation. However, it is in good agreement with a recent paper by Ham,[15] where it is shown that a dynamical Janh-Teller effect may lead to a depression of the spin-orbit coupling. If we neglect the spin-orbit interaction, we may suppress the whole spin space and work only in orbital space.[16] This will be done in the following formulation.

We first combine the degenerate wave functions of a configuration in free space in such a way that they are properly symmetrized in the crystal field of C_{2v} symmetry. This is the normal zero-order approximation of static crystal-field theory. We write $\Psi_{n\alpha\Gamma}{}^{(i)}(r)$, where Γ refers to the group representation to which the total wave function (excepting the spin part) Ψ belongs, α to the parity of the state and n to all other quantum numbers, whereas i indicates the parent configuration. Although C_{2v} has no inversion symmetry, we may ascribe a parity α to the chosen wave functions, because the parent configurations i belong to full rotation symmetry. The wave functions are assumed to be eigenfunctions of the undisturbed Hamiltonian H_0 of the free ion:

$$H_0\Psi_{n\alpha\Gamma}{}^{(i)} = E^{(i)}\Psi_{n\alpha\Gamma}{}^{(i)}, \tag{13}$$

where $E^{(i)}$ is the configurational energy. The perturbation is given by[1,2]

$$V(r,q) = V^{(c)}(r) + \sum_{s\gamma} V^{(s\gamma)}(r) q_{s\gamma} + \cdots, \tag{14}$$

where $V^{(c)}(r)$ is the static crystal field and $q_{s\gamma}$ one of the vibrational coordinates which belongs to the irreducible representation γ of C_{2v}. (The index s here refers to all vibrational modes with the symmetry γ, and should not be confused with the spin quantum number s used in Sec. I.) In terms of the perturbation (14), we may readily calculate the electronic energies in first-order approximation. For $q_{s\gamma}=0$, we have

$$E_{n\alpha\Gamma}{}^{(i)} = E^{(i)} + \langle in\alpha\Gamma | V^{(c)} | in\alpha\Gamma \rangle. \tag{15}$$

Let us now suppose that one of the energies, say $E_{nu\Gamma}{}^{(1)} \equiv E_1$ of the configuration $4f^6 4f^*$ is almost degenerate with one of the energies of the configuration $4f^6 5d$, say $E_{ng\Gamma}{}^{(2)} \equiv E_2$, i.e.,

$$E_1 \approx E_2. \tag{16}$$

Here u and g refer to odd and even parity, respectively. If we now permit $q_{s\gamma}$ to be finite, the effect of (14) will be to produce a strong mixing of both states:

$$E^{(\pm)}(q) = \tfrac{1}{2}\{E_1 + E_2 + \sum_{s\gamma} [V_{11}{}^{(s\gamma)} + V_{22}{}^{(s\gamma)}] q_{s\gamma} \pm [(E_2 - E_1 + \sum_{s\gamma} [V_{22}{}^{(s\gamma)} - V_{11}{}^{(s\gamma)}] q_{s\gamma})^2 + 4(V_{12}{}^{(c)} + \sum_{s\gamma} V_{12}{}^{(s\gamma)} q_{s\gamma})^2]^{1/2}\}, \tag{17}$$

where the matrix element $V_{kl}{}^{(\kappa)}$ have the meaning

$$V_{kl}{}^{(\kappa)} = \langle k\alpha n\Gamma | V^{(\kappa)} | ln'\alpha'\Gamma' \rangle.$$

We will discuss the importance of Eq. (17) for the vibrational problem in the next section. It has been originally derived in a fundamental paper by Neumann and Wigner[5] and it demonstrates that two electronic eigenvalues depending on one adiabatic parameter (in our case a vibrational coordinate q) cannot cross each other, i.e., they cannot become exactly degenerate, except if there is the possibility of a symmetry degeneracy, which however is not the case in C_{2v} symmetry. It is this fact, which distinguishes our problem from the Jahn-Teller case and which will allow us a much simpler theoretical formulation.

If two vibrational coordinates are operative, say q_{A_1} and q_{B_1} and $V_{12}{}^{(s\gamma)}$ is real, then the potential sheets of the coupled states may come together *at one single point.* (If $V_{12}{}^{(s\gamma)}$ is a complex quantity, three vibrational coordinates have to be operative for an intersection at one single point.[5]) But this may be considered unimportant, since each of the sheets represents an infinity-squared manifold of points, so that a single touching point has no practical influence on the quantum mechanical problem. This situation is quite different from the case for which both sheets intersect in a whole (one-dimensional) line, which itself represents an infinite manifold of points.

If only one vibrational coordinate is operative, such that $q_{s\gamma} \equiv q$, we find that the smallest distance between

[13] B. R. Judd, Phys. Rev. **125**, 613 (1962).
[14] H. A. Jahn and E. Teller, Proc. Roy. Soc. (London) **A161**, 22 (1937).
[15] F. S. Ham, Phys. Rev. **138**, A1727 (1965).
[16] It should be emphasized that this can also be done for the ground state because it is an S state (see Sec. I).

the eigenvalues $E^{(+)}$ and $E^{(-)}$ is

$$(E^{(+)}-E^{(-)})_{\min}=2\frac{(E_2-E_1)V_{12}-(V_{22}-V_{11})V_{12}^{(c)}}{[(V_{22}-V_{11})^2+4|V_{12}|^2]^{1/2}} \quad (18)$$

which is reached, if q takes the value:

$$q_{\min}=-\frac{(E_2-E_1)(V_{22}-V_{11})+4V_{12}V_{12}^{(c)}}{(V_{22}-V_{11})^2+4|V_{12}|^2}. \quad (19)$$

In both formulas we have omitted the index $s\gamma$.

(c) *Electron-Lattice Dynamics*

So far the vibrational coordinates $q_{s\gamma}$ have been considered as parameters for the electronic problem. This procedure is justified only if the electronic velocities are considerably greater than those of the nuclei of the lattice, and if the separation of any one electronic state from any neighboring one is larger than one typical vibrational quantum. In this case the Born-Oppenheimer approximation[17] can be employed. However, if two electronic states $E_1(q)$ and $E_2(q)$ approach each other more closely than a typical quantum $\hbar\omega_{s\gamma}$ or even cross each other, as in the pure Jahn-Teller case, then the Born-Oppenheimer approximation breaks down and the theoretical formulation becomes more complicated. This latter problem has been investigated by many authors. We refer the reader to the paper of Ham[15] and to the review article of Longuet-Higgins.[18]

In our case the two electronic states $E^{(+)}$ and $E^{(-)}$ of Eq. (17) *cannot* cross each other if only one vibrational coordinate is operative, and if we postulate that they stay apart from each other by more than one vibrational quantum $\hbar\omega$, such that [see Eq. (18)]:

$$\left|2\frac{(E_2-E_1)V_{12}-(V_{22}-V_{11})V_{12}^{(c)}}{[(V_{22}-V_{11})^2+4|V_{12}|^2]^{1/2}}\right|>\hbar\omega, \quad (20)$$

then the Born-Oppenheimer approximation remains a good approximation. Equation (20) cannot be justified directly because at the present time too little is known about the details of the crystal field and the electronic states. Thus, we adopt it as a postulate of our theory.

Again, if more than one oscillator is coupled to the electronic states, then the point manifold of the sheets $E^{(\pm)}(q)$ in q space is at least an infinity-squared times larger than that of the intersection, so that the intersection may be averaged out in a statistical sense. Thus, our central postulate (20) may be taken to apply to that vibrational mode which is coupled most strongly. This will become clearer in the following discussion.

As a direct consequence of the Born-Oppenheimer approximation, the electronic terms $E^{(+)}(q)$ and $E^{(-)}(q)$ are parts of the potential energy for the oscillators:

$$U^{(\pm)}(q)=\tfrac{1}{2}\sum_{s\gamma}\omega_{s\gamma}{}^2q_{s\gamma}{}^2+E^{(\pm)}(q). \quad (21)$$

[17] M. Born and J. R. Oppenheimer, Ann. Physik **84**, 457 (1957).
[18] H. C. Longuet-Higgins, Advan. Spectry. **2**, 429 (1961).

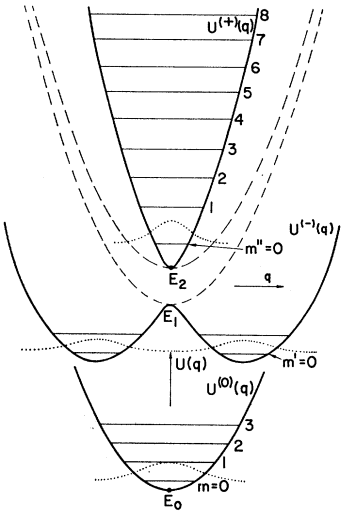

FIG. 4. Potential energy of a single oscillator for the electronic ground state and two almost degenerate excited states. Special case: $V_{11}=V_{22}=V_{12}^{(c)}=0$.

Figure 4 demonstrates the behavior of the potential energy of one single oscillator ($q_{s\gamma}\equiv q$) for the electronic ground state and the two excited states $E^{(\pm)}(q)$ and for the special case $V_{11}=V_{22}=0$, $V_{12}^{(c)}=0$. [We have also assumed that the electronic ground state $E^{(0)}(q)$ is independent of q, which is in agreement with our discussion in Sec. I.] Once these potential energy curves are known, the vibronic states are immediately evident. Let us, therefore discuss (21) for our special case in more detail. The following matrix elements are relevant:

$$V_{11}^{(s\gamma)}=\langle 1nu\Gamma|V^{(s\gamma)}|1nu\Gamma\rangle, \quad (22a)$$

$$V_{22}^{(s\gamma)}=\langle 2n'g\Gamma'|V^{(s\gamma)}|2n'g\Gamma'\rangle, \quad (22b)$$

$$V_{12}^{(s\gamma)}=\langle 1nu\Gamma|V^{(s\gamma)}|2n'g\Gamma'\rangle, \quad (22c)$$

$$V_{12}^{(c)}=\langle 1nu\Gamma|V^{(c)}|2n'g\Gamma'\rangle. \quad (23)$$

$V^{(c)}(r)$ belongs by definition to an A_1 representation in r space. $V^{(s\gamma)}(r)$ is that part of the total interaction potential between the electrons of the defect and the ions of the lattice, which pertains to the linear coupling term

$$\sum_{s\gamma}V^{(s\gamma)}(r)q_{s\gamma}$$

of Eq. (14). It is well known from the theory of the static Jahn-Teller effect,[14] that $V^{(s\gamma)}(r)$ is a basis to the same representation γ in r space as in $q_{s\gamma}$ in q space.

Remembering that C_{2v} symmetry has only one-dimensional representations, we recognize at once that

$$V_{11}^{(s\gamma)}=V_{22}^{(s\gamma)}=0 \quad \text{of} \quad \gamma\neq A_1. \quad (24)$$

Considering the matrix element (23) we see that two cases may be distinguished; namely, the case $\Gamma=\Gamma'$ and the case $\Gamma\neq\Gamma'$. To simplify the discussion we take into account that there exists only two important pseudolocalized modes, for which (see Refs. 1 and 2)

$$s\gamma=A_1,B_1 \quad (25)$$

and for which the vibrational frequency is approximately the same.

Then, for $\Gamma=\Gamma'$, we have

$$V_{11}^{(B_1)}=V_{22}^{(B_1)}=0, \quad V_{12}^{(B_1)}=0. \tag{26}$$

Therefore, according to (17) and (21), there is no coupling whatsoever to the B_1 mode. The potential curves for the A_1 mode in the excited state are altered strongly and are no longer parabola. But even if it were possible in this way to account for the observed strongly increased effective frequency ω_{ab}, it is not possible to simultaneously explain the smaller frequency ω_{ab}'. This case evidently cannot account for all of the experimental results.

The case $\Gamma\neq\Gamma'$ is only interesting if

$$[\Gamma\times\Gamma']=B_1. \tag{27}$$

Otherwise, there would again be the coupling to the A_1 mode only, which is not of interest as just noted above. If (27) is valid, however, we have

$$V_{11}^{(B_1)}=V_{22}^{(B_1)}=V_{12}^{(A_1)}=0; \quad V_{12}^{(e)}=0 \tag{28}$$

and the potential energies (21) take the following form:

$$\begin{aligned}U^{(\pm)}(q_{A_1},q_{B_1})=&\tfrac{1}{2}\omega_{A_1}{}^2q_{A_1}{}^2+\tfrac{1}{2}\omega_{B_1}{}^2q_{B_1}{}^2\\&+\tfrac{1}{2}\{E_1+E_2+(V_{11}^{(A_1)}+V_{22}^{(A_1)})q_{A_1}\\&\pm[[E_2-E_1+(V_{22}^{(A_1)}-V_{11}^{(A_1)})q_{A_1}]^2\\&+4|V_{12}^{(B_1)}|^2q_{B_1}{}^2]^{1/2}\}.\end{aligned} \tag{29}$$

This behavior is shown in Fig. 5. The explanation of Fig. 1 is easily given in terms of Fig. 5, if we assume that absorptive (and emissive) transitions to the lower excited state are weak and providing that the matrix element $V_{12}^{(B_1)}$ is much larger than $V_{11}^{(A_1)}$ and $V_{22}^{(A_1)}$. We will justify these assumptions in the next section. Under these assumptions, the effective vibrational frequency ω_{B_1}'' for the upper excited state is increased strongly over that of the ground state. Moreover, as there is no linear displacement for the B_1 mode, the oscillator wave functions alternate between purely even and purely odd functions. For transitions from the ground state the selection rule

$$m_{B_1}''\rightarrow m_{B_1}=0, \quad \pm2, \quad \pm4,\cdots \tag{30}$$

therefore applies, where the vibrational quantum numbers m have the meaning of Figs. 4 and 5. We see from Eq. (29) that a linear displacement of the A_1 mode does occur, so that transitions to all m_{A_1}'' states are allowed. The low-temperature absorption spectra should, therefore, result from the transitions:

$$\begin{aligned}m_{B_1}=m_{A_1}=0\rightarrow\ & m_{B_1}''=0,m_{A_1}''=0,1,2,3,\cdots,\\ \rightarrow\ & m_{B_1}''=2,m_{A_1}''=0,1,2,3,\cdots,\\ \rightarrow\ & m_{B_1}''=4,m_{A_1}''=0,1,2,3,\cdots,\\ & \text{etc.}\end{aligned} \tag{31}$$

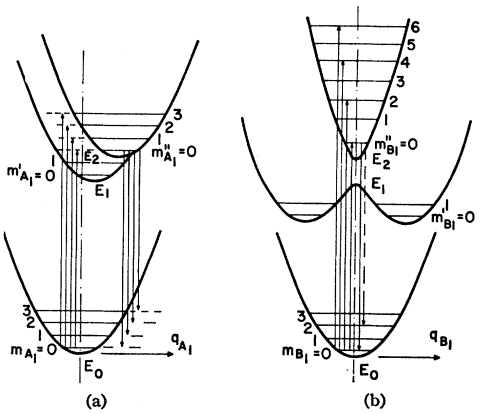

FIG. 5. Potential wells for the two pseudolocalized vibrations A_1 (part a) and B_1 (part b) which are coupled to the electronic states in the system KCl:Eu^{2+}. For part (a) it is assumed that $q_{B_1}=0$, and for part (b) that $q_{A_1}=0$. The displacement of the excited state in part (a) is exaggerated for illustrative purposes. The real displacement, as noted in the text, is such that the first quantum line is most intense.

Accordingly, the strong lines of Fig. 1 represent the transitions

$$m_{A_1}=m_{B_1}=0\rightarrow m_{A_1}''=0,m_{B_1}''=0,2,4,6,\cdots$$

and therefore,

$$2\omega_{B_1}''=\omega_{ab}(\approx4\omega_{B_1}), \tag{32}$$

where ω_{ab} is given in Fig. 1. The interval ω_{ab} decreases monotonically, which is clear from Eq. (29) or from the top curve of Fig. 5(b). The smaller lines within the intervals ω_{ab} represent the transitions $m_{A_1}=m_{B_1}=0\rightarrow m_{B_1}''=0$, $m_{A_1}''=1, 2, \cdots$ and therefore

$$\omega_{A_1}=\omega_{A_1}''=\omega_{ab}. \tag{33}$$

In addition, the emission spectrum may be explained by Fig. 5, if we assume that the emitting state is $m_{A_1}''=m_{B_1}''=0$. From Fig. 5(b), it is clear that the oscillator wave function for the states $m_{B_1}=0$ and $m_{B_1}''=2$ overlap more strongly than those of the states $m_{B_1}=2$ and $m_{B_1}''=0$. Thus the transition $m_{A_1}''=m_{B_1}''=0\rightarrow m_{A_1}=0$, $m_{B_1}=2$ is much weaker than $m_{A_1}''=0$, $m_{B_1}''=0\rightarrow m_{A_1}=0$, $m_{B_1}=0$. Therefore the first emission sequence

$$m_{A_1}''=m_{B_1}''=0\rightarrow m_{B_1}=0, \ m_{A_1}=0,1,2,\cdots \tag{34}$$

is much stronger than the second one, the first line of which, $m_{A_1}''=m_{B_1}''=0\rightarrow m_{B_1}=2$, $m_{A_1}=0$ has approximately the same energy as the line $m_{A_1}''=m_{B_1}''=0\rightarrow m_{A_1}=2$, $m_{B_1}=0$, since $\omega_{A_1}\approx\omega_{B_1}$ (see Refs, 1, 2). The line intervals of the sequence (34) lead to the normal frequency ω_{A_1}. (The second A_1 frequency of Refs. 1, 2 is discernible in Fig. 1, but this is of minor importance in the present context.)

(*d*) *Matrix Elements and Transition Probabilities*

It is shown in Ref. 2 that, for rare-earth (RE) ions in the alkali halides, $V^{(\sigma\gamma)}(r)$ is essentially proportional to

the electric field of the electronic charge distribution of the RE ion. Hence, we may develop $V^{(s\gamma)}(r)$ into a multipole series

$$V^{(s\gamma)}(r)=M^{(s\gamma)}(r)+D^{(s\gamma)}(r)+Q^{(s\gamma)}(r)+\cdots. \quad (35)$$

If we choose the normal coordinates so that the equilibrium of the ground state occurs at $q_{s\gamma}=0$, then it can be shown[2] that the monopole part $M^{(s\gamma)}(r)$ has no influence whatsoever on Eqs. (17) and (29). Now the matrix element over the dipolar part of $V^{(s\gamma)}(r)$

$$\langle in\alpha\Gamma|D^{(s\gamma)}|i'n'\alpha'\Gamma'\rangle \quad (36)$$

is equal to zero if $\alpha=\alpha'$; and the matrix element over the quadrupolar part

$$\langle in\alpha\Gamma|Q^{(s\gamma)}|i'n'\alpha'\Gamma'\rangle \quad (37)$$

is equal to zero if $\alpha\neq\alpha'$. This stems from the fact that $D^{(s\gamma)}$ and $Q^{(s\gamma)}$ have odd and even parity, respectively. Let us now investigate those matrix elements for which Eq. (27) is valid, i.e., $[\Gamma\times\Gamma']=B_1$. Then from (28), (36), and (37) only the following may be nonzero

$$V_{11}^{(A_1)}=\langle 1nu\Gamma|Q^{(A_1)}|1nu\Gamma\rangle, \quad (38a)$$

$$V_{22}^{(A_1)}=\langle 2n'g\Gamma'|Q^{(A_1)}|2n'g\Gamma'\rangle, \quad (38b)$$

$$V_{12}^{(B_1)}=\langle 1nu\Gamma|D^{(B_1)}|2n'g\Gamma'\rangle. \quad (38c)$$

Since we may expect that the quadrupolar coupling is weaker than the dipolar one, i.e.,

$$V_{12}^{(B_1)}|\gg|V_{11}^{(A_1)}|,|V_{22}^{(A_1)}| \quad (39)$$

we may neglect the A_1 terms of Eq. (29), in determining the potential energy for the B mode, which becomes

$$U^{(\pm)}(q_{B_1})=\tfrac{1}{2}\omega_{B_1}{}^2q_{B_1}{}^2 \pm[(E_2-E_1)^2+4|V_{12}^{(B_1)}|^2q_{B_1}]^{1/2}. \quad (40)$$

This directly evinces the increase of the effective B_1 frequency in the upper electronic state $E^{(+)}$, as shown in Fig. 5(b). Because of (39), this increase is quite large for the lower vibrational B_1 states, whereas for the higher ones ω_{B_1}'' approaches ω_{B_1} monotonically, which is demonstrated by the monotonic decrease of the interval ω_{ab} in Fig. 1.

We have not yet explained why the transition from the ground state to the lower one of the excited electronic states $E^{(-)}$ is negligible compared to that of the $E^{(+)}$ states. In the appendix we evaluate the pertinent electric-dipole transition probabilities, and show that the transition probability to the $E^{(-)}$ state is smaller by a factor of approximately 40 than that to the $E^{(+)}$ state. This accounts for the fact that these transitions are not observed in the absorption spectra. A similar argument applies to the emission spectra.

CONCLUSION

We have shown that the anomalously large line interval within a vibrational series in the absorption spectra of Eu^{2+} in the alkali chlorides, can be accounted for in detail through a vibrational coupling of two nearly degenerate electronic states of opposite parity. Since the defect symmetry permits only nondegenerate states, a theorem by Neumann and Wigner requires that any two such states may not cross each other under variations of one of the vibrational coordinates. However, these two states may approach each other and be strongly mixed by the vibrations. Accordingly, under a central postulate of this work, that the eigenvalues of the pertinent states do not approach each other by less than a typical vibrational quantum, the vibrational potential associated with the electronic states of the defect may be determined.

It is found that the electronic ground state is only weakly coupled to the two important pseudolocalized vibrational modes of A_1 and B_1 symmetry. On the other hand, the two nearly degenerate excited electronic states are so strongly coupled to these modes, that for the higher energy state the frequency of the B_1 mode is markedly increased, whereas for the A_1 mode there occurs a displacement of the vibrational coordinate without a change in frequency. In addition, we find a selection rule $\Delta m_{B_1}=0,\pm2,\cdots$ for transitions to this state from the ground state. Thus the strong absorption lines of Fig. 1 with the anomalously high line interval, ω_{ab}, should result from allowed transitions to excited states of the altered B_1 mode, whereas the less intense lines, which lie between the strong lines, should result from transitions to excited states of the normal A_1 mode. It is also shown that the lines of the emission spectrum must again have the regular interval given by the normal A_1 mode. The transition probability between the electronic ground state and the lower energy excited state is found to be small, so that transitions between these states cannot be observed either in absorption or in emission. Many features of the anomalous spectra of Eu^{2+} in the alkali chlorides are thereby accounted for.

It is perhaps worthwhile to speculate at this point on why the pseudo-Jahn-Teller effect is not observed in Eu^{2+}:KBr and Eu^{2+}:KI. Two extremes of the vibrational coupling of electronic states can be discerned. One is the true Jahn-Teller effect, i.e., the case where the electronic states are spatially degenerate. Vibrational coupling is known to play an important role for degenerate (or almost degenerate) states. Nevertheless, the effects of such coupling on the vibrational spectrum are not easily detectable, since the vibrational frequencies in absorption and emission are essentially the same,[6] and the selection rule $\Delta m=0,\pm2,\cdots$ for vibrational transitions found in the present work does not generally apply. The other extreme, is the case of nearly degenerate states which are, however, separated in energy by a sufficiently large amount so that the vibrational coupling is very weak. The change in the vibrational frequency in this case is, of course, small

and again difficult to detect. In between these extremes, is the case assumed to exist for Eu^{2+} in the alkali chlorides. That is, two electronic states exist whose energies are sufficiently close so that a strong vibrational coupling results, but are no closer than one quantum of the pseudolocalized mode. If the energy interval required for this case to apply is small, then we can begin to expect a difference in the vibrational coupling for the states of Eu^{2+} in the alkali chlorides compared to the alkali bromides and iodides. As can be seen in Table I, the pseudolocalized vibrational frequency ω_1 is approximately 200 cm^{-1}, and does not differ among the alkali chlorides by more than 5%. Whereas ω_1 for the bromides and iodides differs from that of the chlorides by approximately 50% and 60%, respectively. Providing, therefore, that the energy difference between the pure electronic states does not also change by proportionate amounts, we might expect a marked difference in the electron-lattice coupling for Eu^{2+} among the alkali halides. A more exact formulation of the criterion for the detectability of the pseudo-Jahn-Teller-effect deserves further study.

APPENDIX

We need to evaluate the electric-dipole transition probabilities for transitions between the ground state $E^{(0)}$ and the excited states $E^{(-)}$ and $E^{(+)}$. We have defined, in Sec. IIb, the E_1 state to belong to the $4f^6 4f^*$ configuration to which the transition probability is small. In contrast, the transition probability to the state E_2, belonging to the $4f^6 5d$ configuration, is strong. Let us assume that

$$E_1 < E_2 \tag{41}$$

as indicated in Figs. 4 and 5. To calculate the electronic transition probabilities, we require the electronic wave functions $\Psi^{(\pm)}(r,q)$. First-order perturbation theory yields

$$\Psi^{(\pm)}(r,q) = C_1^{(\pm)}(q)\Psi_1(r) + C_2^{(\pm)}(q)\Psi_2(r), \tag{42}$$

where, if we neglect $V_{11}^{(A_1)}$ and $V_{22}^{(A_1)}$,

$$\begin{aligned} C_1^{(\pm)}(q_{B_1}) &= V_{12}^{(B_1)} q_{B_1}/N^{(\pm)}, \\ C_2^{(\pm)}(q_{B_1}) &= [(E_2-E_1) \pm E'']/2N^{(\pm)}, \qquad (43) \\ N^{(\pm)} &= \{\tfrac{1}{2}E''[E'' \pm (E_2-E_1)]\}^{1/2}, \qquad (44) \end{aligned}$$

and

$$E'' = [(E_2-E_1)^2 + 4|V_{12}^{(B_1)}|^2 q_{B_1}^2]^{1/2}. \tag{45}$$

It is evident that $C_1^{(\pm)}(q_{B_1})$ is an odd function of q_{B_1}, whereas $C_2^{(\pm)}(q_{B_1})$ is even.

Let us now discuss the transitions to both excited electronic states, $\Psi^{(\pm)}(r,q)$. Since Ψ_0 and Ψ_1 belong to the same configuration, the electronic matrix elements for transitions from the ground state reduce to

$$\int \Psi_0^*(r) r_i \Psi^{(\pm)}(r,q)\,dr = C_2^{(\pm)}(q_{B_1}) \int \Psi_0^*(r) r_i \Psi_2(r)\,dr. \tag{46}$$

From Figs. 4 and 5(b), we see that the potential curve for the lower excited state has minima at, say, $\pm a_{B_1}$ which are displaced from the origin. Thus the state with quantum number $m_{B_1}'=0$ will be centered about these minima. On the other hand, $C_2^{(-)}=0$ for $q_{B_1}=0$ and, therefore we may approximate $C_2^{(-)}(q_{B_1})$ in a simple way

$$C_2^{(-)}(q_{B_1}) \approx C_2^{(-)}(a_{B_1})(q_{B_1}/a_{B_1}). \tag{47}$$

The vibrational wave function for this state $\Phi_{m'=0}^{(-)}$, may be approximated by

$$\Phi_0^{(-)}(q_{B_1}) = (1/\sqrt{2})[\Phi_0^{(-)}(q_{B_1}-a_{B_1}) + \Phi_0^{(1)}(q_{B_1}+a_{B_1})]. \tag{48}$$

The relevant matrix element has been evaluated elsewhere[19] to be

$$\int \Phi_0^{(0)*}(q_{B_1}) q_{B_1} \Phi_0^{(-)}(q_{B_1}-a_{B_1})\,dq_{B_1} = \tfrac{1}{2} a_{B_1} \exp\left[-\frac{a_{B_1}^2 \omega_{B_1}}{4\hbar}\right] \equiv I_{00}. \tag{49}$$

Hence the total probability for the transition $E^{(0)}$, $m_{A_1}=m_{B_1}=0 \rightarrow E^{(-)}$, $m_{A_1}'=m_{B_1}'=0$ is given by

$$P_{E^{(0)},0,0;E^{(-)},0,0} \approx 2|C_2^{(-)} I_{00}|^2 \langle \Psi_0 | r_i | \Psi_2 \rangle. \tag{50}$$

For the upper excited electronic state $E^{(+)}$, on the other hand, the vibrational ground state is centered around $q_{B_1}=0$, and therefore, we may take

$$C_2^{(+)}(q_{B_1}) \approx 1, \tag{51}$$

whereas, the relevant vibrational matrix element is given by[19]

$$\int \Phi_0^{(0)}(q_{B_1})^* \Phi^{(+)}(q_{B_1})\,dq_{B_1} = \left[\frac{2\omega_{B_1}\omega_{B_1}''}{\omega_{B_1}^2 + \omega_{B_1}''^2}\right]^{1/2}. \tag{52}$$

Hence, the total probability for the transition E_0, $m_{A_1}=m_{B_1}=0 \rightarrow E^{(+)}$, $m_{A_1}''=m_{B_1}''=0$ is

$$P_{E^{(0)},0,0;E^{(+)},0,0} \approx \frac{2\omega_{B_1}\omega_{B_1}''}{\omega_{B_1}^2 \omega_{B_1}''^2} |\langle \Psi_0 | r_i | \Psi_2 \rangle|^2. \tag{53}$$

To make a numerical estimate we assume the mean-square displacement for $m_{B_1}''=2$ to be

$$\langle q_{B_1}^2 \rangle_{av} = (5/2)(\hbar/2\omega_{B_1}) \tag{54}$$

[19] M. Wagner, Z. Naturforsch. **14a**, 81 (1959).

which is in agreement with Fig. 1 (i.e., $\omega_{B_1}''=2\omega_{B_1}$). For this displacement, the potential energy should be $(5/4)\hbar(2\omega_{B_1})$ and therefore, we have the requirement

$$\tfrac{1}{2}\omega_{B_1}{}^2\langle q_{B_1}{}^2\rangle_{\rm av}+\tfrac{1}{2}[(E_2-E_1)^2+4|V_{12}{}^{(B_1)}|^2\langle q_{B_1}{}^2\rangle_{\rm av}]^{1/2} -\tfrac{1}{2}(E_2-E_1)=(5/4)\hbar(2\omega_{B_1}) \quad (55)$$

which follows from Eq. (40). Furthermore, we may take the value

$$E_2-E_1\approx\hbar\omega_{B_1} \quad (56)$$

which is a lower limit of our postulate (20). Thus we get from (54) and (55)

$$|V_{12}{}^{(B_1)}|^2/(\hbar\omega_{B_1})^2=4.5(\omega_{B_1}/\hbar). \quad (57)$$

The position $q_{B_1}=a_{B_1}$ of the minimum for the lower excited state is given by

$$a_{B_1}=V_{12}{}^{(B_1)}/\omega_{B_1}{}^2 \quad (58)$$

or, using (57)

$$a_{B_1}{}^2=4.5(\hbar/\omega_{B_1}). \quad (59)$$

Using the Eqs. (54) to (59) and (43), we have

$$|C_2{}^{(-)}(a_{B_1})|^2=0.39, \quad (60)$$

and consequently

$$\frac{P_{E^{(0)},0,0;E^{(-)},0,0}}{P_{E^{(0)},0,0;E^{(+)},0,0}}\approx\frac{1}{40}. \quad (61)$$

Hence, the lines of the transition $E^{(0)}\rightarrow E^{(-)}$ are much weaker than those of the transition $E^{(0)}\rightarrow E^{(+)}$ and this explains why they do not appear in the absorption spectra of Fig. 1. A similar, though more involved, argument shows that the transition probability for the emissive transitions from $E^{(-)}$ to $E^{(0)}$ are much weaker than those from $E^{(+)}$ to $E^{(0)}$.

PHYSICAL REVIEW VOLUME 145, NUMBER 2 13 MAY 1966

Intrinsic Luminescence of RbI and KI at 10°K*

J. RAMAMURTI AND K. TEEGARDEN
Institute of Optics, University of Rochester, Rochester, New York
(Received 17 December 1965)

Emission and excitation spectra for the intrinsic luminescence of RbI and KI have been measured at 10°K and compared with the exciton spectra of the two materials. Two emission bands appear at 3.31 and 4.15 eV for KI, and three for RbI at 2.64, 3.15, and 3.95 eV. Each band has a distinctive excitation spectrum. The high-energy band in each material appears to be connected either with interband transitions or excitation of the $n=2$ Wannier exciton line, while the low-energy emission is associated with absorption in or near the first exciton line. Evidence is given for the existence of a third component of the Wannier exciton series observed recently by Fischer and Hilsch.

INTRODUCTION

IT is known that transitions to exciton states and the conduction band of the alkali iodides result in efficient luminescence at low temperatures.[1] Initial investigations on this intrinsic luminescence have shown that the emission is associated with the recombination of an electron with a trapped hole.[2] Recently, Kabler,[3] and Murray and Keller[4] have presented evidence that the hole trap involved in the luminescence of KI is the well-known V_k center[5] or $I_2{}^-$-molecule ion. In the present paper some details of the excitation and emission spectrum of the intrinsic luminescence of both KI and RbI are presented. An attempt is made to relate the excitation spectra with specific electronic transitions known to occur in these crystals.

For the purposes of this discussion, a brief description of the absorption spectra of KI and RbI is necessary. The absorption spectrum of a thin film of RbI at 10°K is shown in Fig. 1.[6] According to one interpretation,[7] the sharp lines at 5.74 and 6.65 eV are probably due to transitions from the p^6 ground-state configuration of the iodide ion to a configuration in which the excited electron has a wave function with cubic symmetry. Using atomic notation, we may designate this as a suitably modified p^5s configuration. Two lines appear because of the spin-orbit interaction of the hole in the p^5 core of the iodide ion. The two additional lines at 6.49 and 6.98 eV probably occur because of transitions to a p^5d-like configuration which may be split into several states because of the cubic crystal field. Spin-orbit splitting would further increase the number of possible states due to this configuration. These strong absorption

* Supported in part by the U. S. Army Research Office, Durham, North Carolina.
[1] K. J. Teegarden, Phys. Rev. **105**, 1222 (1957).
[2] K. Teegarden and R. Weeks, J. Phys. Chem. Solids **10**, 211 (1959).
[3] M. N. Kabler, Phys. Rev. **136**, A1296 (1964).
[4] R. B. Murray and F. J. Keller, Phys. Rev. **137**, A942 (1965).
[5] T. G. Castner and W. Kanzig, J. Phys. Chem. Solids **3**, 178 (1957).
[6] G. Baldini and K. J. Teegarden (to be published).
[7] R. S. Knox and N. Inchauspe, Phys. Rev. **116**, 1093 (1959).